Numerical modelling of magnetic characteristics of ferrite core taking account of both eddy current and displacement current

Mohendro Kumar Ghosh [a],[*], Yanhui Gao [a], Hiroshi Dozono [a], Kazuhiro Muramatsu [a], Weimin Guan [b], Jiaxin Yuan [b], Cuihua Tian [b], Baichao Chen [b]

[a] Department of Electrical and Electronic Engineering, Saga University, Saga 840-8502, Japan
[b] School of Electrical Engineering, Wuhan University, Wuhan 430072, PR China

ABSTRACT

In the magnetic field analysis of magnetic devices using a ferrite core, such as a pulse transformer, the frequency-domain analysis is often carried out using the measured complex permeability under different frequency range. However, the nonlinear magnetic characteristics cannot be considered in the frequency-domain analysis because of the harmonics caused by it cannot be represented. The nonlinear magnetic characteristics can be considered in the time-domain analysis, but suitable constant conductivity and permittivity taking account of the microstructure of ferrite core, which can represent the measured complex permeability under different frequencies, needs to be investigated for the time-domain analysis. In this paper, the effective permeability of a toroidal ferrite core is tried to be demonstrated by using the linear ac steady state magnetic field analysis taking account eddy currents and displacement currents. It is shown that the measured permeability can be realized roughly by using the modified constant conductivity and permittivity. The nonlinear time-domain magnetic field analysis can be carried out using the modified constant conductivity and permittivity obtained from this paper.

1. Introduction

Ferrite cores are widely used in transformers and inductors, etc. for high frequency electronic devices because of high magnetic permeability and low conductivity [1, 2, 3, 4]. In the magnetic field analyses of such magnetic devices using a ferrite core, the frequency-domain analysis is often carried out using the measured complex permeability under different frequencies. However, the harmonics caused by the magnetic nonlinearity of the ferrite core cannot be evaluated by using the frequency-domain analysis. The nonlinear magnetic characteristics can be considered in the time-domain analysis, but suitable frequency-free conductivity and permittivity for the time-domain analysis, which can represent the measured complex permeability under different frequencies, need to be investigated. In [1, 2], a coupled magnetic-circuit analysis is proposed taking account of the microstructure of ferrite core using a simple equivalent RC circuit. However, the conductivity and permittivity obtained are frequency dependent, which cannot be used in the time-domain analysis with multi-frequencies.

In this paper, we tried to obtain suitable frequency-free conductivity and permittivity using a simple linear ac steady state magnetic field analysis taking account of eddy currents and displacement currents. The effective permeability of a toroidal ferrite core is tried to be demonstrated by using the simple finite element magnetic field analysis taking account of eddy currents and displacement currents. The suitable constant conductivity and permittivity, which can realize the measured complex permeability of the toroidal Mn–Zn ferrite core under various frequencies in the catalog data [5], are obtained and tried to be explained.

2. Model

In this paper, the complex permeability in the catalog of the toroidal Mn–Zn ferrite core (TDK/EPCOS: T37) as shown in Fig. 1 [5] is tried to be reproduced using modified constant conductivity and permittivity. The complex permeability is obtained by using the measured impedance, the effective magnetic length, number of turns, and the sectional area of the core (IEC 62044-1), with frequency below 10 MHz and maximum flux density below 0.25 mT.

---

* Corresponding author.
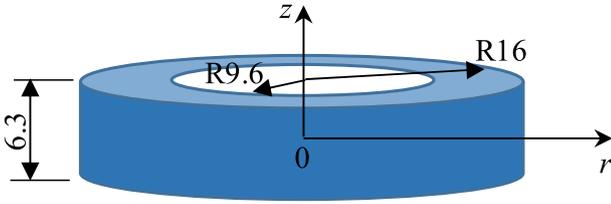 E-mail address: 16694907@edu.cc.saga-u.ac.jp (M.K. Ghosh).

Fig. 1. Dimensions of the toroidal ferrite core for the measurement.

3. Materials and methods

3.1. Analysis model

Fig. 2 shows the axisymmetric analysis model of the toroidal ferrite core shown in Fig. 1. Only half region is analyzed due to symmetry. Only one layer of air with thickness of 0.1 mm is added outside the ferrite core to calculate the effective complex permeability. The permittivity in the air is set to be zero neglecting the displacement currents in the air. The surface layer of core is subdivided into 0.01 mm to represent the skin effect appropriately. The original permeability μ_{so} of the ferrite core is set to be 6100 referring to the real permeability μ_s' at 10 kHz because the imaginary permeability μ_s'', which is generated by hysteresis phenomena and eddy current effect, is relatively small and can be neglected at 10 kHz. The original conductivity σ_o and original permittivity ε_{so} are set to be 5 S/m and $300\varepsilon_0$ (ε_0 is the permittivity in vacuum.) following the catalog. The conductivity and permittivity are adjusted to realize the frequency characteristic of the complex permeability.

3.2. Method of magnetic field analysis

The ac linear steady state magnetic field analysis taking account of eddy current and displacement current [6] is carried out using the A method (A: magnetic vector potential) with the first order square edge finite element method and the phasor method. The fundamental equation is shown as follows:

$$\text{rot } (\nu \text{ rot } \dot{A}) = -j\omega\sigma\dot{A} + \omega^2\varepsilon\dot{A} \tag{1}$$

where ν is reluctivity, ε is permittivity, σ is conductivity, and ω is angular frequency. The superscript (˙) denotes the complex variable. The first term in the right-hand side is the eddy current and the second term is the displacement current. Only r and z components A_r and A_z, respectively, of A are unknowns and the magnetic flux density of 0.1mT is applied in θ direction by using Dirichlet boundary conditions, following the measured conditions of B less than 0.25mT.

3.3. Effective complex permeability

The effective complex permeability $\dot{\mu}$ is calculated using the following equation.
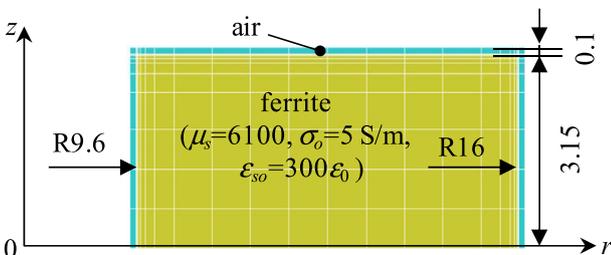
$$\dot{\mu} = \frac{\dot{B}_f}{\dot{H}_a} = \frac{\sum\limits_{ie=1}^{N_f} \dot{B}^{(ie)} \cdot S^{(ie)} \left/ \sum\limits_{ie=1}^{N_f} S^{(ie)} \right.}{\sum\limits_{je=1}^{N_a} \dot{H}^{(je)} \cdot S^{(je)} \left/ \sum\limits_{je=1}^{N_a} S^{(je)} \right.} \tag{2}$$

where B_f is the average flux density in the ferrite core and H_a is the average magnetic field intensity in the air corresponding to the applied magnetic field because eddy currents in the core do not affect the magnetic field in the air. N_f and N_a are the numbers of elements of the ferrite core and the air, respectively. S denotes the area. The calculation method of complex permeability using B and H matches with the measurement method in principle, in which the complex permeability is calculated by using the measured impedance, namely, voltage and current.

4. Study area

4.1. Original material constant

First, the magnetic field analysis taking account of eddy currents and displacement currents is carried out using the original conductivity σ_o and permittivity ε_{so}.

The flux, eddy current, and displacement current distributions at $\omega t = 0$ and -90 deg. at frequency $f = 100$ MHz are shown in Figs. 3, 4, and 5, respectively. Strong skin effect is observed in the flux, eddy current, and displacement distributions. The eddy currents are larger than displacement currents even if f is 100 MHz.

Fig. 6 shows the calculated complex permeability under various frequencies. The tendency of the calculated permeabilities are similar with the catalog data. Namely, both the catalog and calculated μ_s' do not change in lower frequency region and they decrease in higher frequency region. Moreover, both the catalog and calculated μ_s'' increase in lower frequency region and they decrease in higher frequency region. However, the peak positions are shifted and the gradients are different from each other. Therefore, to realize the real frequency characteristics of the complex permeability, the conductivity and permittivity should be changed.
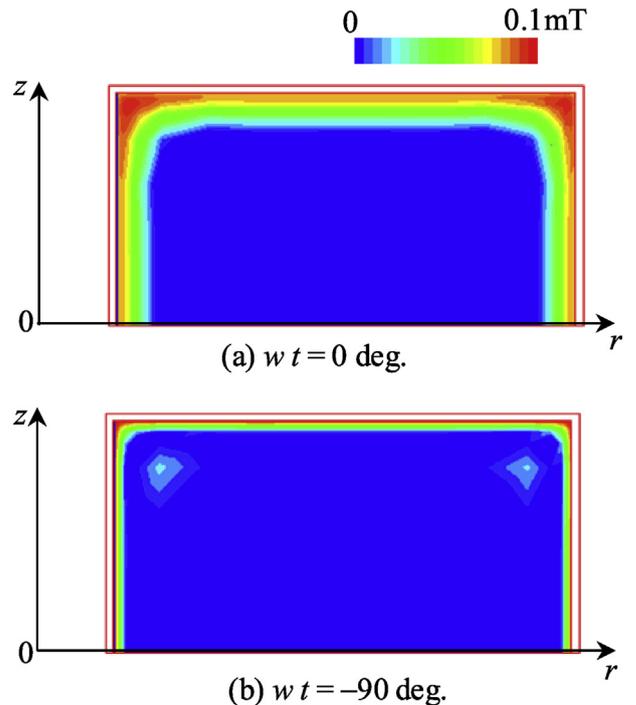

Fig. 2. Axisymmetric analysis model (half region).

Fig. 3. Flux distributions ($\sigma = \sigma_o$, $\varepsilon_s = \varepsilon_{so}$, $f = 100$ MHz).

(a) $wt = 0$ deg.

(b) $wt = -90$ deg.
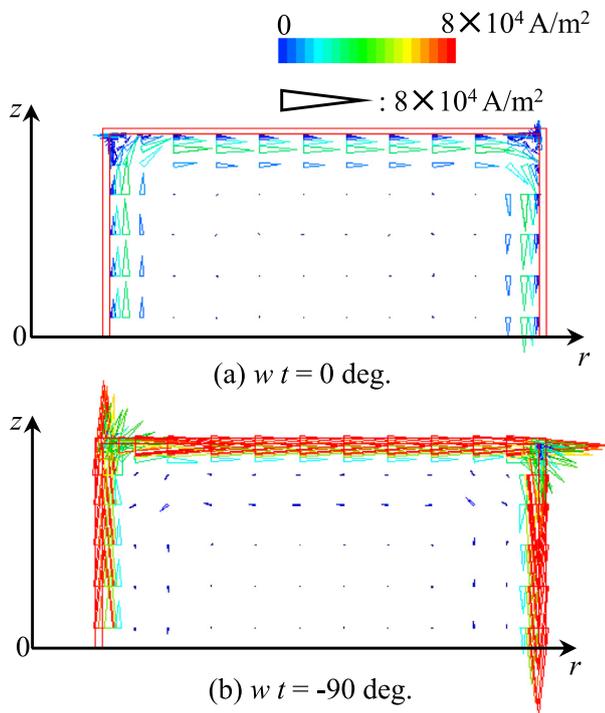
Fig. 4. Eddy current distributions ($\sigma = \sigma_o$, $\varepsilon_s = \varepsilon_{so}$, $f = 100$ MHz).

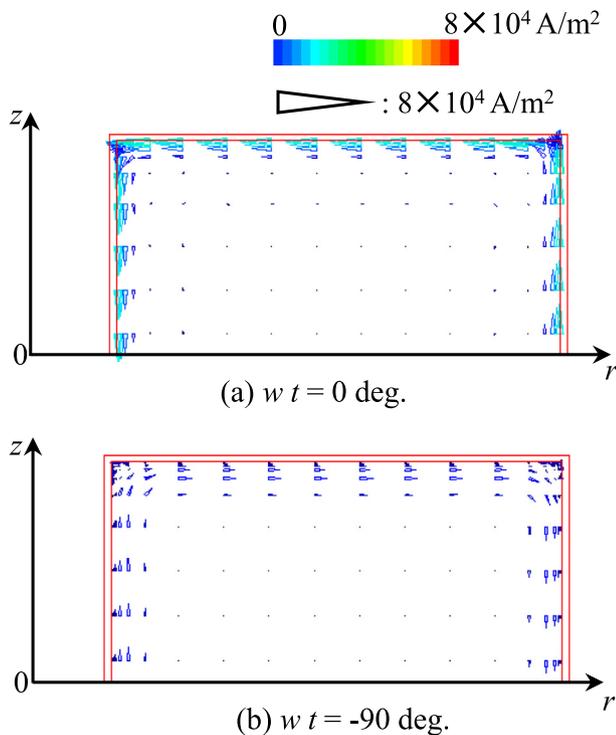(a) $wt = 0$ deg.

(b) $wt = -90$ deg.

Fig. 5. Displacement current distributions ($\sigma = \sigma_o$, $\varepsilon_s = \varepsilon_{so}$, $f = 100$ MHz).

4.2. Modified conductivity model with only eddy current

Then, to investigate the effect of the conductivity on the characteristics of the complex permeability, the model with only eddy current, in which the displacement current is neglected ($\varepsilon_s = 0$) is carried out and the conductivity σ is modified to be 10 times of the original one. The
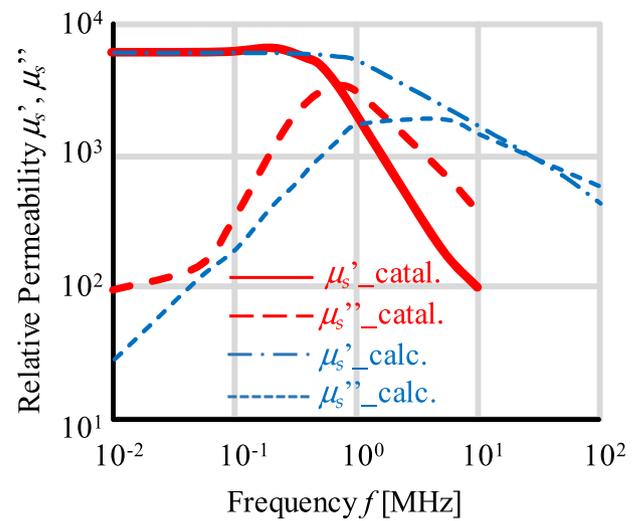

Fig. 6. Complex relative permeability with original material constant ($\sigma = \sigma_o$, $\varepsilon_s = \varepsilon_{so}$).

calculated complex permeabilities with $\sigma = \sigma_o$ and $10\sigma_o$ are shown in Fig. 7.

When the conductivity is $10\sigma_o$, μ_s' starts to decrease at lower frequency than the case of σ_o, so the peak position of μ_s' can be realized by choosing an appropriate value of conductivity, however, the gradient at high frequency region does not change. Moreover, the peak position of μ_s'' can be changed but the peak value and gradient of μ_s'' cannot be changed by adjusting σ. Therefore, the model with only eddy current cannot represent the real frequency characteristics of the complex permeability.

4.3. Modified permittivity model

Next, the effect of permittivity on the characteristics of complex permeability is investigated. The permittivity is varied with $\sigma = \sigma_o$ because μ_s'' becomes zero if only the displacement current was considered ($\sigma = 0$). The calculated complex permeabilities with $\varepsilon_s = \varepsilon_{so}$ and $100\varepsilon_{so}$ are shown in Fig. 8.

When the permittivity is $100\varepsilon_{so}$, just complementary to the case of changing the conductivity, the frequency at which μ_s' starts to decrease cannot be changed but the gradient can be changed. Moreover, also complementary to the case of changing the conductivity, the peak position of μ_s'' cannot be changed but the peak value and gradient of μ_s'' can be changed by adjusting ε_s. Therefore, it is possible to represent the real characteristics of complex permeability by changing σ and ε_s simultaneously.

4.4. Modified conductivity and permittivity model

According to the results shown above, both the conductivity and permittivity are modified to represent the real characteristics of the complex permeability. Fig. 9 shows the complex permeability with $\sigma = 4\sigma_o$ and $\varepsilon_s = 400\varepsilon_{so}$ obtained by using the error and correction method. The real characteristics of the complex relative permeability can be reproduced overall by choosing the above optimal value for σ and ε_s, respectively. The catalog data of the complex relative permeability of a Ni–Zn ferrite core (TDK/EPCOS: M13) is also tried to be reproduced by using the same method and the results are shown in Fig. 10. The modified conductivity $\sigma = 4.0 \times 10^6 \sigma_o$ and permittivity $\varepsilon_s = 1.2 \times 10^5 \varepsilon_{so}$ are very large compared with the original ones, whereas the complex relative permeability can be almost represented.
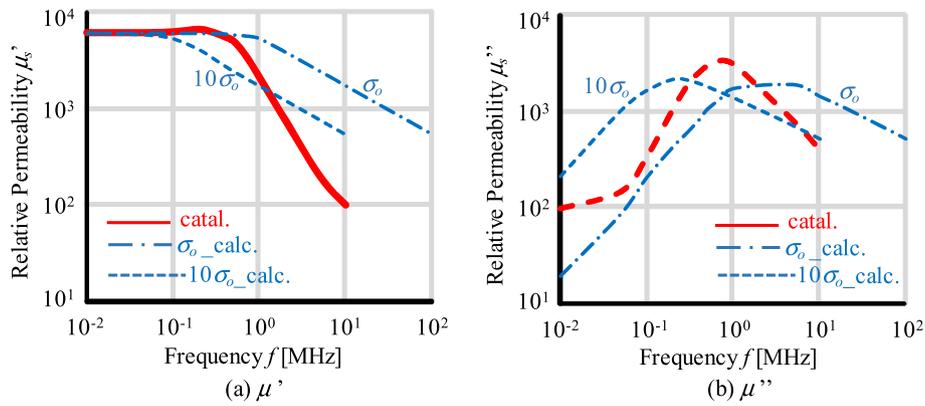
Fig. 7. Complex relative permeability with modified conductivity ($\varepsilon_s = 0$).
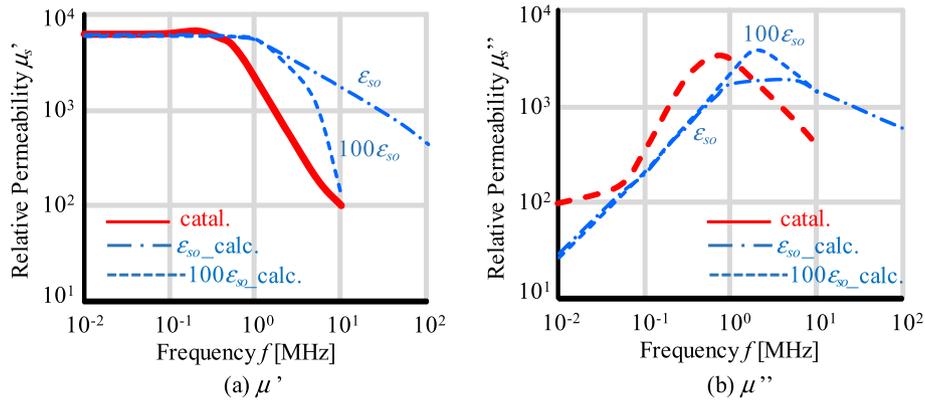

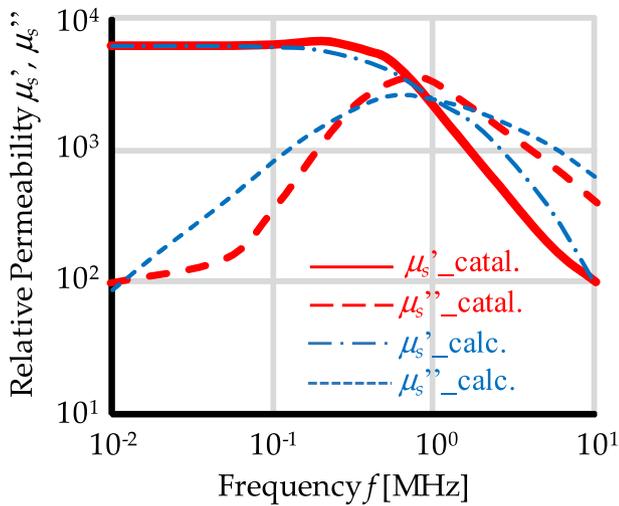**Fig. 8.** Complex relative permeability with modified permittivity model ($\sigma = \sigma_o$).

Fig. 9. Complex relative permeability with modified conductivity and permittivity model ($\sigma = 4\sigma_o$, and $\varepsilon_s = 400\,\varepsilon_{so}$).
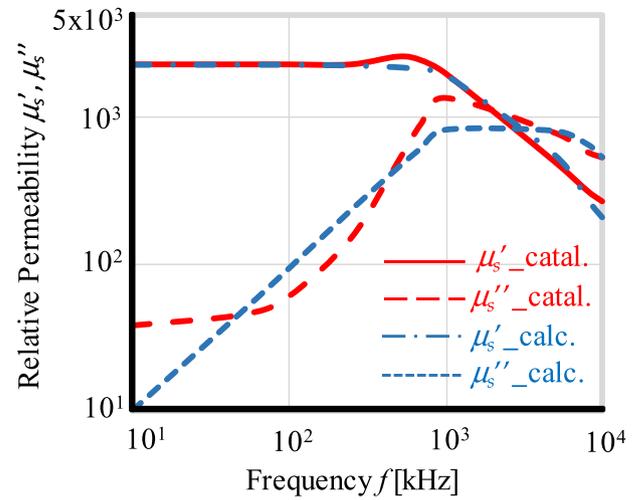

Fig. 10. Complex relative permeability with modified conductivity and permittivity model ($\sigma = 40\text{x}10^5\sigma_o$, and $\varepsilon_s = 1.2\text{x}10^4\,\varepsilon_{so}$) with Ni–Zn material.

5. Discussion

The effectiveness of obtaining the constant optimal values for $\sigma = 4\sigma_o$ and $\varepsilon_s = 400\varepsilon_{so}$ of Mn–Zn ferrite are tried to be explained by using a simplified microstructure of a homogeneous model of ferrite core containing the dielectric effect of a crystalline grain boundary as shown in Fig. 11. An equivalent RC circuit [1] can be considered from the homogeneous model as shown in Fig. 11. In the homogeneous ferrite core model, there exist different types of conductivity and permittivity such as

conductivity in the grains, permittivity in the boundary, capacitance in the boundary, etc. which are quite difficult to calculate due to the complex structure of a ferrite core. As a result, the equivalent homogeneous conductivity and permittivity obtained by using the RC circuit are shown in (3) and (4).

$$\sigma(\omega) = \frac{\sigma_g \omega^2 \varepsilon_s^2 + \sigma_g \sigma_b (\sigma_g + \sigma_b)}{\left(\frac{L}{D^2}\right)\omega^2 \varepsilon_s^2 + \left(\frac{L}{D^2}\right)(\sigma_g + \sigma_b)^2} \tag{3}$$
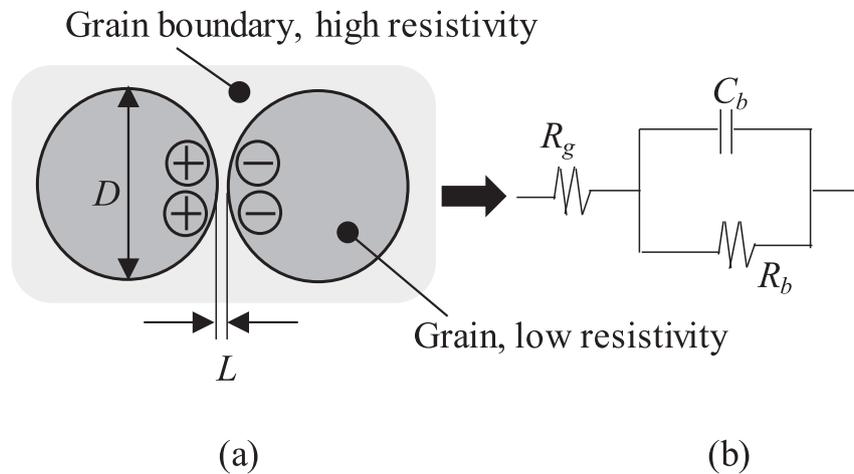
Fig. 11. Conceptual diagram of the microstructure of Mn–Zn ferrite (a) homogeneous model and (b) equivalent RC circuit.

Table 1
Parameters list used in analysis.

Name	Symbol	Value
Conductivity in grains	σ_g	$100\Omega^{-1}m^{-1}$
Conductivity in grain boundary layers	σ_b	$2.6 \times 10^{-5}\Omega^{-1}m^{-1}$
Grain size	D	$9 \times 10^{-6}m$
Boundary layer thickness	L	$1 \times 10^{-16}m$
Dielectric constant	$\varepsilon/\varepsilon_0$	0.1

frequency and permittivity versus frequency characteristics obtained by using (3) and (4) from the homogeneous ferrite model and the equivalent *RC* circuit. It shows that the obtained relative conductivity and permittivity are $4\sigma_o$ and $380\varepsilon_{so}$ respectively, and they are constant in a wide frequency region up to 100 MHz range which can make a clear validation and interpretation of Fig. 11 and Fig. 12. So, the obtained suitable constant values for relative conductivity ($4\sigma_o$) and relative permittivity ($400\varepsilon_{so}$) can be considered to realize the complex relative permeability
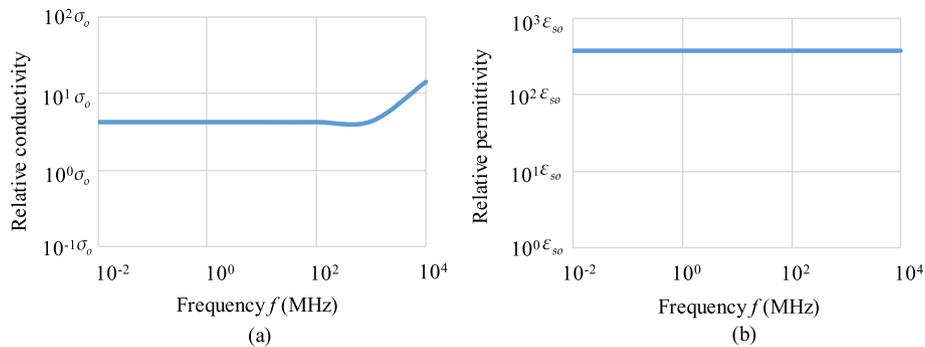

Fig. 12. (a) Conductivity and (b) relative permittivity versus frequency.

$$\varepsilon(\omega) = \frac{\sigma_g^2 \varepsilon_s \left(\frac{D^2}{L}\right)}{\omega^2 \varepsilon_s^2 + \left(\sigma_g + \sigma_b\right)^2} \qquad (4)$$

in which σ_g is the conductivity of the grains, σ_b is the conductivity of the grain boundary, and C_b is the capacitance of the grain boundary. C_b is approximated by using $\varepsilon D^2/L$, in which D is the grain size and L is the boundary layer thickness. Also, dielectric constant ($\varepsilon/\varepsilon_0$) is set to reproduce complex relative permeability in the lower frequency region where the dimensional effects is negligible. A larger value is assumed for σ_g because of the high conductivity in the grain and a smaller value is chosen for σ_b due to the low conductivity in the grain boundary [1]. By choosing the appropriate values for D and L in a reasonable range, the constant frequency free conductivity and permittivity can be obtained by using (3) and (4). Generally, ferrite cores are found frequency dependent [1, 2]. But sometime ferrite cores show frequency independent characteristics due to its unique material properties, considering displacement current in magnetic field analysis, pattern of equations obtained from equivalent circuit, etc. Table 1. shows the parameters list used in analysis with respective determined values. Fig. 12 shows the conductivity versus

characteristics up to 10 MHz.

6. Conclusion

The simple analysis method taking account of both eddy current and displacement current using constant conductivity and permittivity to represent the real frequency characteristics of complex relative permeability of the ferrite core is proposed. It is shown that, the proposed modified constant conductivity and permittivity can be used to represent the real frequency characteristics of the complex relative permeability roughly. In future, the time-domain analysis taking account of the nonlinear magnetic characteristics of the ferrite core can be carried out using the modified constant conductivity and permittivity obtained from this paper.

Declarations

Author contribution statement

Mohendro Kumar Ghosh: Analyzed and interpreted the data; Contributed reagents, materials, analysis tools or data; Wrote the paper.

Yanhui Gao: Conceived and designed the experiments; Performed the experiments.

Hiroshi Dozono, Jiaxin Yuan: Conceived and designed the experiments.

Kazuhiro Muramatsu: Conceived and designed the experiments; Analyzed and interpreted the data; Contributed reagents, materials, analysis tools or data.

Weimin Guan: Performed the experiments.

Cuihua Tian: Analyzed and interpreted the data.

Baichao Chen: Contributed reagents, materials, analysis tools or data.

Competing interest statement

The authors declare no conflict of interest.

Additional information

No additional information is available for this paper.

References

[1] A. Furuya, Y. Uehara, K. Shimizu, J. Fujisaki, T. Ataka, T. Tanaka, H. Oshima, Magnetic field analysis for dimensional resonance in Mn-Zn ferrite toroidal core and comparison with permeability measurement, IEEE Trans. Magn. 53 (11) (January 2017).

[2] F. Fiorillo, C. Beatrice, O. Bottauscio, E. Carmi, eddy-current losses in Mn-Zn ferrites, IEEE Trans. Magn. 50 (1) (January 2014).

[3] F.G. Brockman, P.H. Dowling, W.G. Steneck, Dimensional effects resulting from a high dielectric constant found in a feromagnetic ferrite, Phys. Rev. 77 (January 1950) 85–93.

[4] D. Zhang, C.F. Foo, Effect of high permeability on the accurate determination of permeability of permittivity for Mn-Zn ferrite cores, IEEE Trans. Magn. 40 (6) (November 2004).

[5] https://en.tdk.eu/tdk-en/.

[6] S. Sudo, K. Muramatsu, K. Yamazaki, T. Ueda, "Basic Study on Method of Calculating Impedance of Concrete Taking into Account Displacement Current," the Papers of Technical Meeting on Static Apparatus and Rotating Machinery of IEE Japan, SA-06-29, RM-06-29, 2006 (in Japanese).